

# Infrared spectrum of $^{16}\text{O}^{18}\text{O}^{16}\text{O}$ in the 5 $\mu\text{m}$ range. Positions, intensities, and atmospheric applications

M.R. De Backer-Barilly, A. Barbe, and V.I.G. Tyuterev

*Groupe de Spectrometrie Moleculaire et Atmospherique, Reims, France*

Received January 16, 2003

The absorption of various  $^{18}\text{O}$  enriched isotopomers of ozone has been reinvestigated in the 2000–2250  $\text{cm}^{-1}$  spectral range. This work has allowed for the first time to observe of  $2\nu_1$  (221 transitions) and  $2\nu_3$  (414 transitions) weak bands of  $^{16}\text{O}^{18}\text{O}^{16}\text{O}$ . This leads to the determination of the Hamiltonian parameters for the three (002), (101), (200) interacting states and a very satisfactorily rms errors ( $0.77 \cdot 10^{-3} \text{ cm}^{-1}$ ) in the line positions. In addition, relative intensities, measured for the three bands lead to transition moment operators. Both results allow to perform calculations of the complete list of  $^{16}\text{O}^{18}\text{O}^{16}\text{O}$  lines reported in the S&MPO bank. This is of direct interest for atmospheric applications, as the  $\nu_1 + \nu_3$  band of the  $^{16}\text{O}^{18}\text{O}^{16}\text{O}$  isotopomer, clearly observed in balloon or satellites spectra, interferes with the strong  $\nu_3$  band of OCS, used for atmospheric retrievals.

## Introduction

Pursuing the systematic study of the ozone molecule in the infrared, including isotopic species, we have recently published<sup>1</sup> the line positions of many bands of  $^{16}\text{O}^{18}\text{O}^{16}\text{O}$  between 700 and 5000  $\text{cm}^{-1}$ . But the 5  $\mu\text{m}$  spectral range, where the main  $\nu_1 + \nu_3$  band appears, was not revised. The analysis of this band has been published<sup>2</sup> earlier, but the interacting  $2\nu_1$  and  $2\nu_3$  bands were not observed at that time and no data on the intensities have been reported.

The main reason is the extreme complexity of analyzing the spectra. In generating  $^{18}\text{O}$  enriched ozone, the six forms appear ( $^{16}\text{O}_3$ ,  $^{16}\text{O}^{16}\text{O}^{18}\text{O}$ ,  $^{16}\text{O}^{18}\text{O}^{16}\text{O}$ ,  $^{18}\text{O}^{18}\text{O}^{16}\text{O}$ ,  $^{18}\text{O}^{16}\text{O}^{18}\text{O}$ , and  $^{18}\text{O}_3$ ), which leads to very crowded spectra. In the corresponding energy range, four vibrational states (002), (030), (101), and (200) interact for each isotopomer, in such a way that 24 bands have to be analyzed in a total and the number of observed transitions is of the order of 10 000 lines in a 250  $\text{cm}^{-1}$  interval.

Thanks to a long experience of analyzing ozone spectra that gives us *a priori* knowledge of the various resonances and their consequences on the intensity redistribution, and thanks to very good predictions of band centers<sup>3,4,5</sup> (better than 0.1  $\text{cm}^{-1}$  in this spectral range) and rotational constants<sup>6,7</sup> we have finally been able to assign all the transitions observed in the six isotopic species.

We report here the analysis of the  $2\nu_3$ ,  $\nu_1 + \nu_3$ , and  $2\nu_1$  bands of the  $^{16}\text{O}^{18}\text{O}^{16}\text{O}$  isotopomer, both for rovibrational line positions and intensities. This analysis is directly helpful for atmospheric purposes, as many publications<sup>8,9,10</sup> show atmospheric spectra with features assigned to this isotopic species.

## Experimental setup

The experimental setup has been described in earlier published papers by our group<sup>11,12</sup> and related

information is available in the internet accessible S&MPO system at two websites: <http://ozone.univ-reims.fr> and <http://ozone.iao.ru> (see Ref. 13). Then, we report here only specific remarks for the present analysis.

In the spectra we reported earlier and which were recorded for all isotopomers,<sup>1,7,14–16</sup> with the aim to analyze higher wave number range the product  $p \times L = 10 \text{ Torr} \times 32 \text{ m}$  was too large for the 2000–2150  $\text{cm}^{-1}$  spectral range, therefore most of the lines of the  $\nu_1 + \nu_3$  bands were saturated. Then we have recorded a new set of spectra with 4 meters path length. Let us remind that the first analysis of this region<sup>2</sup> was obtained using only a 30 cm path length cell. The list of all used spectra is given in Table 1. As has already been explained<sup>14</sup> the use of various mixtures leads to a first determination of the transitions belonging to  $^{16}\text{O}^{18}\text{O}^{16}\text{O}$  and  $^{16}\text{O}^{16}\text{O}^{18}\text{O}$  or  $^{16}\text{O}^{18}\text{O}^{18}\text{O}$  with  $^{18}\text{O}^{16}\text{O}^{18}\text{O}$ .

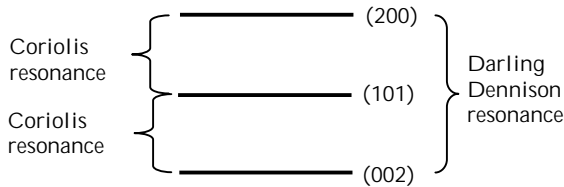
**Table 1. Experimental conditions for recorded spectra**

Isotopomer	Spectrum#1	Spectrum#2	Spectrum#3
	( $L = 31.186 \text{ cm}$ )	( $L = 416.0 \text{ cm}$ )	( $L = 3216.0 \text{ cm}$ )
Pressure, Torr			
$^{16}\text{O}_3$	3.76	5.40	14.55
$^{16}\text{O}^{16}\text{O}^{18}\text{O}$	3.37	3.69	7.06
$^{16}\text{O}^{18}\text{O}^{16}\text{O}$	1.68	1.85	3.53
$^{18}\text{O}^{18}\text{O}^{16}\text{O}$	1.53	1.26	1.71
$^{18}\text{O}^{16}\text{O}^{18}\text{O}$	0.76	0.63	0.85
$^{18}\text{O}_3$	0.36	0.22	0.21

The spectra have been calibrated using  $^{12}\text{C}^{16}\text{O}$  standard lines.<sup>17</sup> The positions of the lines are obtained using a peakfinder included into our multifit program,<sup>18,19</sup> in such a way that the accuracy for each line is of the order of  $3 \cdot 10^{-4} \text{ cm}^{-1}$ . This program is also used to derive the observed intensities of fully isolated transitions belonging only to the  $^{16}\text{O}^{18}\text{O}^{16}\text{O}$  isotopic species.

## Analysis

As was already mentioned, to assign lines of  $^{16}\text{O}^{18}\text{O}^{16}\text{O}$ , it was necessary to analyze simultaneously the three other isotopic species  $^{18}\text{O}^{16}\text{O}^{18}\text{O}$ ,  $^{16}\text{O}^{16}\text{O}^{18}\text{O}$ , and  $^{18}\text{O}^{18}\text{O}^{16}\text{O}$ , as spectra of  $^{16}\text{O}_3$  and  $^{18}\text{O}_3$  are known.<sup>13</sup> Considering the usual ozone polyad scheme,<sup>20,21</sup> we expect the following resonances for  $C_{2v}$  isotopic species:



In addition, the (030) state may perturb the (002) state through anharmonic resonance and the (101) state through Coriolis resonance. We include the (030) state in our analysis only in those cases where related perturbations are clearly observed.

In case of  $C_s$  isotopic species, the situation is more complicated, as anharmonic resonance coupling are allowed between all vibrational states, in addition to the above mentioned resonances. This problem does not concern the  $^{16}\text{O}^{18}\text{O}^{16}\text{O}$  analysis, but it was necessary to take it into account for a correct assignment of interfering  $^{16}\text{O}^{16}\text{O}^{18}\text{O}$  transitions. The analysis of the triad {(002), (101), (200)} (or tetrad including the (030) state) at present is not fully complete for the three other mixed isotopomers, but allows us to trust our analysis of  $^{16}\text{O}^{18}\text{O}^{16}\text{O}$ .

After the assignment of all strongest lines of the other isotopomers (668, 886, and 868), we made, as the first step, calculation of transitions, starting from the initial parameters of the triad {(002), (101), (200)}. The Hamiltonian parameters of (101) state and coupling parameters were those of Ref. 2. We updated new values for rotational constants  $A$ ,  $B$ , and  $C$  for the (030) and (200) states as well as new values corresponding to predictions for performed with new isotopically invariant band centers potential function of the ozone molecule.<sup>5</sup> We also made use of the opportunity to calculate, with our multifit program, synthetic spectra<sup>18,19</sup> for each isotopomer separately or with additional contributions. This enables us to identify clearly the  $2\nu_3$  band and to start the rovibrational assignments. The assignment of the  $2\nu_1$  band was more difficult, as this band is very weak and almost entirely blended by the strongest  $\nu_1 + \nu_3$  bands of  $^{16}\text{O}^{16}\text{O}^{18}\text{O}$  and  $^{16}\text{O}^{16}\text{O}^{16}\text{O}$ . We have succeeded in this assignment by making iteration processes between calculations and assignments. For the 3 bands we have finally assigned 1456 transitions. We report in Table 2, the number of observed transitions, as well as their rotational quantum numbers range, compared with those of the previous study of the  $\nu_1 + \nu_3$  band.<sup>2</sup> For the lines observed in this study, we did not see significant perturbations due to possible resonance with the (030) state. The latter state has not been then used in our analysis.

**Table 2. The number of transitions observed and the range of quantum number variations**

Parameter	(002)	(101)	(200)	Ref.
$J_{\max}$	56	60	47	Present study
	—	43	—	2
$K_a \max$	17	18	12	Present study
	—	13	—	2
Number of transitions	414	821	221	Present study
	—	353	—	2

The effective Hamiltonian used is the same as in various references<sup>22,23</sup>: diagonal vibration blocks  $H^{VV}$  have usual Watson form<sup>22</sup>

$$\begin{aligned} \langle V | H | V \rangle = & E^{VV} + \left[ A - \frac{1}{2} (B + C) \right] J_z^2 + \\ & + \frac{1}{2} (B + C) J^2 + \frac{1}{2} (B - C) J_{xy}^2 - \Delta_K J_z^4 - \Delta_{JK} J_z^2 J^2 - \\ & - \Delta_J (J^2)^2 - \delta_K \{ J_z^2, J_{xy}^2 \} - 2\delta_J J_{xy}^2 J^2 + H_K J_z^6 + \\ & + H_{KJ} J_z^4 J^2 - H_{JK} J_z^2 (J^2)^2 + H_J (J^2)^3 + h_K \{ J_z^4, J_{xy}^2 \} + \\ & + h_{KJ} \{ J_z^2, J_{xy}^2 \} J^2 + 2h_J J_{xy}^2 (J^2)^2 + L_K J_z^8, \quad (1) \end{aligned}$$

where the standard notations [...] are used:  $\{A, B\} \equiv AB + BA$  and  $J_{xy}^2 \equiv J_x^2 - J_y^2$ .

For non-diagonal vibrational blocks which describe resonance interactions, we use the same "normal ordering"<sup>23</sup> of ladder components of angular momentum in the molecular fixed frame  $J_{\pm} = J_x \pm \pm (1/i) J_y$  as in our earlier papers and as in the information system "Spectroscopy and Molecular Properties of Ozone" (S&MPO).<sup>13,24,25</sup> Coriolis interaction blocks in this case take the form<sup>23</sup>:

$$\begin{aligned} \langle V | H_{\text{Coriolis}} | V \rangle = & C_{001} (J_+ - J_-) + \\ & + C_{011} (J_+ (J_z + 1/2) + (J_z + 1/2) J_-) + \\ & + C_{021} (J_+ (J_z + 1/2)^2 - (J_z + 1/2)^2 J_-) + \\ & + C_{201} J^2 (J_+ - J_-) + C_{003} (J_+^3 - J_-^3) + \\ & + C_{031} (J_+ (J_z + 1/2)^3 - (J_z + 1/2)^3 J_-) + \\ & + C_{211} J^2 (J_+ (J_z + 1/2) + (J_z + 1/2) J_-) + \dots \quad (2) \end{aligned}$$

and anharmonic interaction blocks are written as

$$\begin{aligned} \langle V | H_{\text{anharmon}} | V \rangle = & F_{001} + F_{020} J_z^2 + \\ & + F_{002} (J_+^2 + J_-^2) + F_{200} J^2 + \dots \quad (3) \end{aligned}$$

The line positions fit is performed using transitions, without weighting function. It leads to the parameters presented in Table 3, with their standard errors. The root mean squares (rms) residual is satisfactory:  $0.77 \cdot 10^{-3} \text{ cm}^{-1}$ . Statistics is given in Table 4.

Table 3. Spectroscopic parameters of the {(002), (101), (200)} triad of states

Parameter	(002)	St. error	(101)	St. error	(200)	St. error
$E^{VV}$	1997.97645 <sub>5</sub>	0.00012	2049.367981 <sub>0</sub>	0.000086	2138.47721 <sub>6</sub>	0.00018
$A - (B + C)/2$	2.786897 <sub>4</sub>	0.000022	2.8293877 <sub>3</sub>	0.0000085	2.875470 <sub>0</sub>	0.000023
$(B + C)/2$	0.410909 <sub>5</sub>	0.000021	0.4122922 <sub>0</sub>	0.0000082	0.413866 <sub>8</sub>	0.000021
$(B - C)/2$	0.026816 <sub>5</sub>	0.000020	0.0265654 <sub>9</sub>	0.0000082	0.026525 <sub>5</sub>	0.000021
$\Delta_K \cdot 10^3$	0.175830 <sub>1</sub>	0.000012	0.182263 <sub>8</sub>	0.000036	0.188515 <sub>2</sub>	0.000045
$\Delta_{JK} \cdot 10^5$	-0.16896 <sub>1</sub>	0.00072	-0.13582 <sub>3</sub>	0.00081	$g$	
$\Delta_J \cdot 10^6$	0.44584 <sub>5</sub>	0.00040	0.46590 <sub>5</sub>	0.00039	0.46278 <sub>7</sub>	0.00075
$\delta_K \cdot 10^5$	0.2869 <sub>6</sub>	0.0043	0.2592 <sub>7</sub>	0.0027	0.4131 <sub>9</sub>	0.0038
$\delta_J \cdot 10^7$	0.8674 <sub>9</sub>	0.0024	0.7232 <sub>7</sub>	0.0021	0.6707 <sub>4</sub>	0.0033
$H_K \cdot 10^7$	$g$		0.30402 <sub>0</sub>	0.00084	$g$	
$H_{KJ} \cdot 10^8$	$g$		-0.1330 <sub>5</sub>	0.0033	$g$	
$H_{JK} \cdot 10^{10}$	$g$		$g$		$g$	
$H_J \cdot 10^{12}$	$g$		$g$		$g$	
$h_K \cdot 10^8$	$g$		$g$		$g$	
$h_{KJ} \cdot 10^{11}$	$g$		$g$		$g$	
$h_J \cdot 10^{12}$	$g$		$g$		$g$	

Parameters of resonance interaction				
Parameter	$\langle 101   H   002 \rangle$		$\langle 101   H   200 \rangle$	
	Value	St. error	Value	St. error
$C_{001}$	-0.2828 <sub>4</sub>	0.0014	0.2959 <sub>2</sub>	0.0011
$C_{011}$	-0.01303 <sub>3</sub>	0.00010	-0.013720 <sub>6</sub>	0.000069
$C_{211} \cdot 10^6$	-0.2528 <sub>5</sub>	0.0028		
$C_{003} \cdot 10^7$	-0.638 <sub>1</sub>	0.086		
	$\langle 200   H   002 \rangle$			
$F_{000}$	-26.8 Ref. 32		-	

Note. The value of  $g$  parameter has been fixed at its value for the ground state.<sup>32</sup> All the values are given in  $\text{cm}^{-1}$ .

Table 4. Statistics on processing the line centers

Vibrational state	rms, $\cdot 10^3 \text{ cm}^{-1}$	$\delta E =  E^{\text{obs}} - E^{\text{calc}} $	Percentage of the total number of lines
(002)	0.92	$\delta E < 0.5 \cdot 10^{-3} \text{ cm}^{-1}$	48.6
		$0.5 \cdot 10^{-3} \text{ cm}^{-1} \leq \delta E < 1 \cdot 10^{-3} \text{ cm}^{-1}$	25.6
		$1 \cdot 10^{-3} \text{ cm}^{-1} \leq \delta E < 2 \cdot 10^{-3} \text{ cm}^{-1}$	22.9
		$2 \cdot 10^{-3} \text{ cm}^{-1} \leq \delta E < 3 \cdot 10^{-3} \text{ cm}^{-1}$	2.4
		$3 \cdot 10^{-3} \text{ cm}^{-1} \leq \delta E < \delta E_{\text{max}}$ $\delta E_{\text{max}} = 4.1 \cdot 10^{-3} \text{ cm}^{-1}$	0.5
(101)	0.67	$\delta E < 0.5 \cdot 10^{-3} \text{ cm}^{-1}$	69.8
		$0.5 \cdot 10^{-3} \text{ cm}^{-1} \leq \delta E < 1 \cdot 10^{-3} \text{ cm}^{-1}$	20.3
		$1 \cdot 10^{-3} \text{ cm}^{-1} \leq \delta E < 2 \cdot 10^{-3} \text{ cm}^{-1}$	8.6
		$2 \cdot 10^{-3} \text{ cm}^{-1} \leq \delta E < 3 \cdot 10^{-3} \text{ cm}^{-1}$	1.0
		$3 \cdot 10^{-3} \text{ cm}^{-1} \leq \delta E < \delta E_{\text{max}}$ $\delta E_{\text{max}} = 5.9 \cdot 10^{-3} \text{ cm}^{-1}$	0.3
(200)	0.85	$\delta E < 0.5 \cdot 10^{-3} \text{ cm}^{-1}$	55.7
		$0.5 \cdot 10^{-3} \text{ cm}^{-1} \leq \delta E < 1 \cdot 10^{-3} \text{ cm}^{-1}$	27.1
		$1 \cdot 10^{-3} \text{ cm}^{-1} \leq \delta E < 2 \cdot 10^{-3} \text{ cm}^{-1}$	14.5
		$2 \cdot 10^{-3} \text{ cm}^{-1} \leq \delta E < 3 \cdot 10^{-3} \text{ cm}^{-1}$	1.8
		$3 \cdot 10^{-3} \text{ cm}^{-1} \leq \delta E < \delta E_{\text{max}}$ $\delta E_{\text{max}} = 4.8 \cdot 10^{-3} \text{ cm}^{-1}$	0.9

Table 5. Comparison between the predicted and experimentally measured band centers

Band	Predicted (Ref. 5)	Observed (this work)	Obs. - Pred. ( $\text{cm}^{-1}$ )	Previous determination (Ref. 2)	Ref. 2 - Pred. ( $\text{cm}^{-1}$ )
$2\nu_3$	1993.024	1993.038 <sub>0</sub>	+0.014	1994.311*	-1.287
$\nu_1 + \nu_3$	2049.375	2049.368 <sub>0</sub>	-0.007	2049.369	-0.006
$2\nu_1$	2143.616	2143.415 <sub>6</sub>	-0.200	2140.326*	+3.290

Note. "Dark" states marked with asterisk have not been observed experimentally in Ref. 2. The global predictions in Ref. 5 were obtained using an isotopically invariant potential function of the molecule.

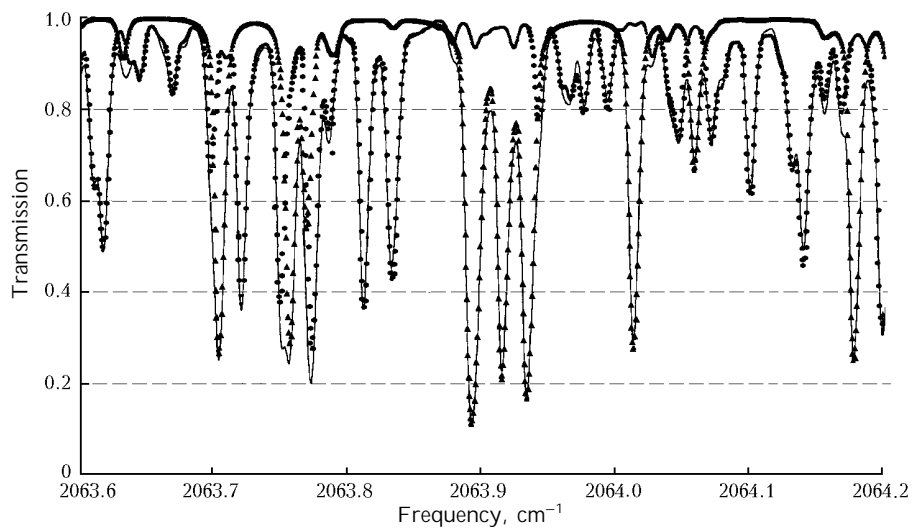


Fig. 1. Contributions from various isotopomers to the observed spectrum in the range of 2064  $\text{cm}^{-1}$ : experiment (solid line); contributions coming from  $^{16}\text{O}_3$ ,  $^{16}\text{O}^{16}\text{O}^{18}\text{O}$ ,  $^{18}\text{O}^{18}\text{O}^{16}\text{O}$ ,  $^{18}\text{O}^{16}\text{O}^{18}\text{O}$ , and  $^{18}\text{O}_3$  isotopomers (dots); contribution from the  $^{16}\text{O}^{18}\text{O}^{16}\text{O}$  isotopomer (triangles).

Table 6. Parameters of the transition moment (D) and statistics of the processed line intensities

Operator	Parameter	Value	Statistics*	
			Deviation, %	Number of intensities
$\varphi_x$	$d_1$	<i>Band</i> $2\nu_3$	$\delta I/I < 2$	119 (53.4%)
		$(0.770_3 \pm 0.014) \cdot 10^{-2}$	$2 \leq \delta I/I < 4$	80 (35.9%)
		<i>Band</i> $2\nu_1$	$4 \leq \delta I/I < 6$	20 (8.9%)
$\varphi_x$	$d_1$	$(-0.1037_2 \pm 0.0042) \cdot 10^{-2}$	$6 \leq \delta I/I \leq 7.4$	4 (1.8%)
$\varphi_z$	$d_1$	$(0.38152_6 \pm 0.00054) \cdot 10^{-1}$		
$1/2 [\{\varphi_x, iJ_y\} + \{i\varphi_y, J_x\}]$	$d_6$	$(0.181_4 \pm 0.055) \cdot 10^{-4}$		

Note. \*  $\delta I/I = |\text{experiment} - \text{calcul.}|/\text{calcul.}$  ( $I$  is line intensity;  $\delta I$  is experimental error in the intensity); rms = 5.9%.

Let us recall that, due to anharmonic resonance (Darling–Dennison) between (200) and (002), the band centers of  $2\nu_1$  and  $2\nu_3$  do not coincide with the vibrational diagonal matrix elements  $E^{VV}$ . These band centers, given in Table 5, are compared with those of Ref. 2 ( $2\nu_1$  and  $2\nu_3$  being not observed) and with the new predictions,<sup>5</sup> which use a new isotopically invariant molecular potential function.

## Intensities

Here we have to address the problems on determination of the amount of the  $^{16}\text{O}^{18}\text{O}^{16}\text{O}$  isotopomer in various cells. To derive the amount of various ozone isotopic species, we use the statistics based on the proportion of oxygen atoms O present in various molecular oxygen  $\text{O}_2$  mixtures. It is now well known that this assumption leads to controversy (Refs. 26, 27, and references therein), nevertheless the maximum error does not exceed 6% in case of  $\text{C}_{2v}$  molecule (Refs. 28, 29, and references therein). In this case, it is clear that we derive "relative intensities" very suitable to reproduce observed laboratory spectra and assign all transitions in atmospheric spectra, but further work is needed to derive the exact amount of the isotopomer in the stratosphere

and then to definitively conclude on the various possible enrichment in the atmosphere.

As explained previously, due to very large number of blended transitions for every isotopomer, only a sample of 223 best transitions have been selected for intensity measurements. These fully unblended lines have been selected with the help of "multifit program"<sup>18,19</sup> by comparing three spectra (see Fig. 1): the first was the observed spectrum, the second was the calculated spectrum of all isotopomers absorbing in the considered spectral range, and the last was the calculated  $^{16}\text{O}^{18}\text{O}^{16}\text{O}$  spectrum. The observed intensities have been derived using the multifit procedure. These experimental intensities are modeled by fitting the parameters involved in the transition moment operator<sup>30</sup> expanded in powers of the elementary rotational operators:

For A type band

$$\begin{aligned}
 {}^{(000)(101)} \tilde{\mu}_z = & d_1 \varphi_z + d_2 \{\varphi_z, J^2\} + d_3 \{\varphi_z, J_z^2\} + \\
 & + d_4 1/2 [\{\varphi_x, iJ_y\} - \{i\varphi_y, J_x\}] + \\
 & + d_5 1/2 [\{\varphi_x, \{J_x, J_z\}\} - \{i\varphi_y, i\{J_y, J_z\}\}] + \\
 & + d_6 1/2 [\{\varphi_x, iJ_y\} + \{i\varphi_y, J_x\}] + d_7 [\{\varphi_x, \{J_x, J_z\}\} + \\
 & + \{i\varphi_y, i\{J_y, J_z\}\}] + d_8 \{\varphi_z, J_{xy}^2\}. \quad (4)
 \end{aligned}$$

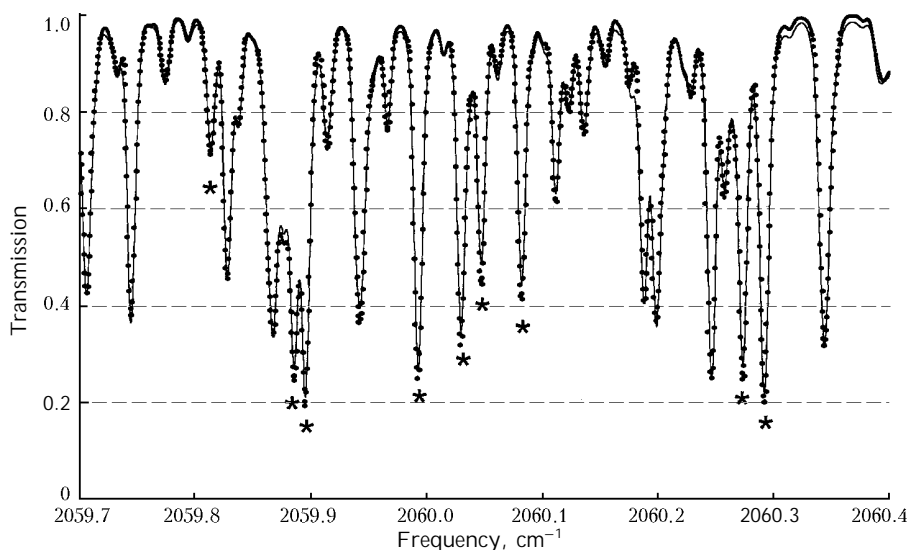


Fig. 2. An example of the final difference between experiment and calculation for the transmission in the region of 2060 cm<sup>-1</sup>: experiment (solid line); calculations (dots).

For B type band

$$\begin{aligned} {}^{(000)(200)}\tilde{\mu}_z = & d_1\varphi_x + d_2\{\varphi_x, J_z^2\} + d_3\{\varphi_x, J_z^2\} + \\ & + d_4\{i\varphi_y, J_z\} + d_5\{\varphi_z, iJ_y\} + d_6\{\varphi_z, \{J_x, J_z\}\} + \\ & + d_7\frac{1}{2}[\{\varphi_x, J_{xy}^2\} + \{i\varphi_y, i\{J_x, J_z\}\}]. \end{aligned} \quad (5)$$

Table 6 represents the parameters of the transition moments operators with the statistics.

Figure 2 shows the agreement between the observed spectrum and the calculated one. Lines marked with the asterisk \* correspond to <sup>16</sup>O<sup>18</sup>O<sup>16</sup>O lines.

## Atmospheric applications and conclusion

A total of 1456 transitions of the 2ν<sub>3</sub>, ν<sub>1</sub> + ν<sub>3</sub>, and 2ν<sub>1</sub> interacting bands of <sup>16</sup>O<sup>18</sup>O<sup>16</sup>O ozone isotopomer have been observed. The first observations of the two weak bands 2ν<sub>1</sub> and 2ν<sub>3</sub> allow a precise determination of Hamiltonian parameters in the usual scheme of interacting polyads.<sup>13,20,21</sup>

With the Hamiltonian parameters (Table 3), and the transition moment operators parameters (Table 6), we have generated a line list for all transitions of the three bands 2ν<sub>3</sub>, ν<sub>1</sub> + ν<sub>3</sub>, and 2ν<sub>1</sub>. This calculation has been performed with a cut-off of 0.3 · 10<sup>-25</sup> cm<sup>-1</sup>/(mol · cm<sup>-2</sup>), up to J = 65 and K<sub>a</sub> = 20. The partition function used in calculations was Z(296 K) = 3599. The integrated band intensity is S(2ν<sub>3</sub>) = 7.61 · 10<sup>-20</sup>, S(ν<sub>1</sub> + ν<sub>3</sub>) = 1.14 · 10<sup>-18</sup>, S(2ν<sub>1</sub>) = 1.99 · 10<sup>-20</sup>, in cm<sup>-1</sup>/(mol · cm<sup>-2</sup>) at T = 296 K. The list of lines will be soon available on the websites S&MPO,<sup>13</sup> in the form directly usable in atmospheric applications. Note that it is important to know the absorption of the <sup>16</sup>O<sup>18</sup>O<sup>16</sup>O isotopomer, as it absorbs in the spectral range of the ν<sub>3</sub> band of the OCS molecule, which basically serves<sup>10</sup> for deriving OCS concentration in the atmosphere.

## References

1. M.-R. De Backer-Barilly, A. Barbe, VI.G. Tyuterev, A. Chichery, and M.-T. Bourgeois, *J. Mol. Spectrosc.* (accepted) (2002).
2. J.-M. Flaud, M.-T. Bourgeois, A. Barbe, J.-J. Plateaux, and C. Camy-Peyret, *J. Mol. Spectrosc.* **165**, 464–469 (1994).
3. VI.G. Tyuterev, S.A. Taskhun, P. Jensen, A. Barbe, and T. Cours, *J. Mol. Spectrosc.* **198**, 57–76 (1999).
4. VI.G. Tyuterev, S.A. Taskhun, D.W. Schwenke, P. Jensen, T. Cours, A. Barbe, and M. Jacon, *Chem. Phys. Lett.* **316**, 271–279 (2000).
5. VI.G. Tyuterev, S.A. Tashkun, D.W. Schwenke, and A. Barbe, in preparation (2003).
6. A. Barbe, A. Chichery, T. Cours, VI.G. Tyuterev, and J.J. Plateaux, *J. Mol. Structure* (Accepted) (2002).
7. A. Chichery, Thesis, Université de Reims, France (2000).
8. D.W. Arlander, A. Barbe, M.-T. Bourgeois, A. Hamdouni, J.-M. Flaud, C. Camy-Peyret, and Ph. Demoulin, *J. Quant. Spectrosc. Radiat. Transfer* **52** No. 3/4, 267–271 (1994).
9. A. Goldman, F.J. Murcray, D.G. Murcray, J.J. Kusters, C.P. Rinsland, J.M. Flaud, C. Camy-Peyret, and A. Barbe, *J. Geophys. Research* **94**, 8467 (1989).
10. G. Toon, Private communication.
11. J.J. Plateaux, A. Barbe, and A. Delahaigue, *Spectrochimica Acta* **51A**, No. 7, 1153–1169 (1995).
12. L. Régalia, Thesis, Université de Reims, France (1996).
13. VI.G. Tyuterev, A. Barbe, Yu.L. Babikov, and S.N. Mikhailenko, in: *XVIIth Colloquium on High Resolution Molecular Spectroscopy*, Nijmegen (2001), paper F28.
14. S.N. Mikhailenko, Yu.L. Babikov, VI.G. Tyuterev, and A. Barbe, in: *MODAS Conference*, Irkutsk (2001), paper 05.1.
15. A. Barbe, S.N. Mikhailenko, VI.G. Tyuterev, and Yu.L. Babikov, in: *HITRAN Conference*, Boston (2002).
16. <http://ozone.univ-reims.fr> and <http://ozone.iao.ru>
17. A. Chichery, A. Barbe, VI.G. Tyuterev, and S. Tashkun, *J. Mol. Spectrosc.* **205**, 347–349 (2001).
18. A. Chichery, A. Barbe, VI.G. Tyuterev, and M.-T. Bourgeois, *J. Mol. Spectrosc.* **206**, 1–13 (2001).
19. A. Chichery, A. Barbe, and VI.G. Tyuterev, *J. Mol. Spectrosc.* **206**, 14–26 (2001).

20. A.G. Maki and J.S. Wells, NIST Special Publications, (1991).
21. J.J. Plateaux, L. Régalia, C. Boussin, and A. Barbe, *J. Quant. Spectrosc. Radiat. Transfer* **68**, 507–520 (2001).
22. C. Boussin, B. Lutz, A. Hamdouni, and C. de Bergh, *J. Quant. Spectrosc. Radiat. Transfer* **63**, 49–84 (1999).
23. J.-M. Flaud and R. Bacis, *Spectrochim. Acta* **V54A**, 3–16 (1998).
24. S.N. Mikhailenko, A. Barbe, V.I. Tyuterev, and A. Chichery, *Atmos. Oceanic Opt.* **12**, No. 9, 771–785 (1999).
25. J.K.G. Watson, *J. Chem. Phys.* **46**, 4189–4196 (1967).
26. V.I. Perevalov and V.I. Tyuterev, *Opt. Spectrosk.* **52**, 644–650 (1982).
27. F. Robert and C. Camy-Peyret, *Annales Geophysicae* **19**, 229–244, (2001).
28. K. Mauersberger, *Geophys. Res. Lett.* **8**, 935 (1981).
29. L.K. Christensen, N.W. Larsen, F.M. Nicolaisen, T. Pedersen, G.O. Sorensen, and H. Egsgaard, *J. Mol. Spectrosc.* **175**, 220–233 (1996).
30. R.W. Larsen, N.W. Larsen, F.M. Nicolaisen, G.O. Sorensen, and J.A. Beukes, private communication.
31. O.N. Sulakshina, Yu.G. Borkov, V.I. Tyuterev, A. Barbe, *J. Chem. Phys.* **113**, No. 23, 10572–10582 (2000).
32. J.-M. Flaud, C. Camy-Peyret, A.N. 'Com, V. Malathy Devi, C.P. Rinsland, and M.A.H. Smith, *J. Mol. Spectrosc.* **133**, 217–223 (1989).